STATISTICAL HADRONIZATION OF MULTISTRANGE PARTICLES*

Michal Petráň[a,b], Jean Letessier[a,c], Vojtěch Petráček[b]
Jan Rafelski[a]

[a]Department of Physics, University of Arizona, Tucson, Arizona 85721, USA
[b]Czech Technical University in Prague
Faculty of Nuclear Sciences and Physical Engineering, Prague, Czech Republic
[c]Laboratoire de Physique Théorique et Hautes Energies
Université Paris 6 et 7, Paris 75005, France

(Received October 25, 2010)

We study multistrange hadrons produced in NA49 and STAR experiments at center of mass energies varying from $\sqrt{s_{NN}} = 7.61$ GeV to 200 GeV. We show that the yields of Ξ, $\overline{\Xi}$ and ϕ can help to constrain the physical conditions present in the hot dense fireball source of these multistrange hadrons created in heavy ion collision. We address the question of chemical equilibrium of individual quark flavors before and after hadronization and offer a few predictions for LHC.

PACS numbers: 24.10.Pa, 12.38.Mh, 25.75.–q, 13.60.Rj

1. Introduction

The Statistical Hadronization Model (SHM) successfully describes particle production in heavy ion collisions for a wide range of reaction energies studied in the past decade at SPS and RHIC, and has been widely accepted as a tool in the analysis of physical phenomena. Special features of multistrange particle yields observed in these experiments inspired this work.

Particular particle ratios are sensitive to the valence quark content of the particles under consideration. For this reason we can explore the hot dense fireball flavor content. We gain insight regarding the mechanisms of QGP breakup by considering how simple assumptions about dynamics of the hadronization alter the result. We extend here our discussion of how the yields of multistrange hadrons can be used in such an analysis [1].

* Lecture presented by Michal Petráň at the L Cracow School of Theoretical Physics "Particle Physics at the Dawn of the LHC", Zakopane, Poland, June 9–19, 2010.

We begin with a summary of experimental results considered in Sec. 2 and introduce the statistical hadronization models in Sec. 3. Our main interest here will be the ratio of $\Xi(ssq)$ to $\phi(\bar{s}s)$, which we address in detail in Sec. 3.3. This experimental data will help us establish that there exists a common set of hadronization conditions for quite different reaction conditions, such as centrality, and collision energy. Based on the universality of SPS and RHIC results we propose in Sec. 4 several predictions for LHC energies.

2. Experimental results

Data of interest for us obtained in Pb–Pb collisions by NA49 Collaboration at SPS and in Au–Au collisions by STAR Collaboration at RHIC are summarized in Table I. Using these results we obtained the generalized ratios of Ξ/ϕ (see Eq. (5)), Ξ/K (see Eq. (8)) and Ξ/π (see Eq. (11)) shown in Fig. 1. We note that the ratio of Ξ/ϕ is practically constant for all systems studied with center of mass energies varying from $\sqrt{s_{NN}} = 7.61$ to 200 GeV and number of participants ranging from $N_{\rm part} \simeq 20$ (most peripheral collisions) to 350 (most central).

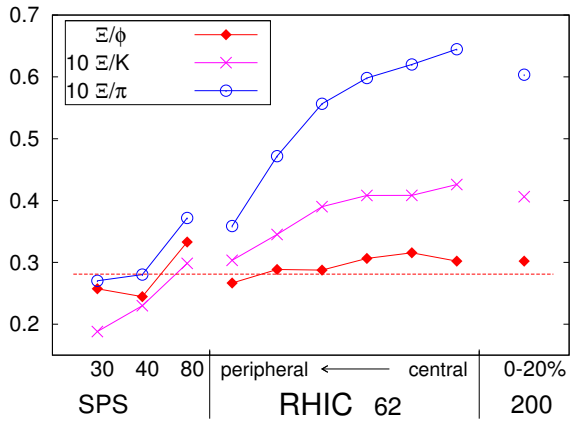

Fig. 1. Data points of Ξ/ϕ Eq. (5), Ξ/K Eq. (8) and Ξ/π Eq. (11). The straight dashed line shows average $\Xi/\phi = 0.281$.

We are in particular interested in recent data from RHIC obtained as a function of centrality at $\sqrt{s_{NN}} = 62.4$ GeV. We performed a centrality dependence study shown in Fig. 2. For every particle species the yield can be interpolated by the following form

$$f(N_{\rm part}) = a\, N_{\rm part}^{b} + c\,. \tag{1}$$

TABLE I

Values for the ratios of Ξ/ϕ Eq. (5), Ξ/K Eq. (8), Ξ/π and ϕ/π Eq. (11) obtained from the experimental data of individual particle yields and the resulting estimated uncertainty in γ_q and γ_s, respectively. Symbol "E" in the error column signals that the particle ratio is the result of the interpolation and/or extrapolation needed to account for different centrality bins.

Experiment	Ref.	Centrality	$10 \times \Xi/\phi$	$\delta\gamma_q$	$10^2 \times \Xi/K$	$\delta\gamma_s$
STAR 62	[2–4]	0–5%	3.04	E	4.19	9.6%
STAR 62	[2–4]	5–10%	3.00	E	4.08	9.2%
STAR 62	[2–4]	10–20%	2.94	E	4.06	9.3%
STAR 62	[2–4]	20–40%	2.88	12.5%	3.79	E
STAR 62	[2–4]	40–60%	2.85	14.6%	3.38	E
STAR 62	[2–4]	60–80%	2.49	19.3%	2.84	E
STAR 200	[2,4,5]	0–20%	3.02	11.8%	4.06	12.9%
SPS 80A	[6–8]	7%	3.33	24.5%	3.04	22.7%
SPS 40A	[6–8]	7%	2.45	42.1%	1.89	18.0%
SPS 30A	[6,7,9]	7%	2.57	66.5%	1.85	24.3%

Experiment	Ref.	Centrality	$10^3 \times \Xi/\pi$	$10 \times \phi/K$	$10^2 \times \phi/\pi$	—
STAR 62	[2–4]	0–5%	6.22	1.38	2.04	—
STAR 62	[2–4]	5–10%	6.20	1.36	2.06	—
STAR 62	[2–4]	10–20%	5.98	1.38	2.04	—
STAR 62	[2–4]	20–40%	5.48	1.32	1.91	—
STAR 62	[2–4]	40–60%	4.65	1.18	1.63	—
STAR 62	[2–4]	60–80%	3.45	1.14	1.38	—
STAR 200	[2,4,5]	0–20%	6.04	1.34	$^*2.54^{+0.21}_{-0.09}$	—
SPS 80A	[6–8]	7%	2.6	0.83	0.88	—
SPS 40A	[6–8]	7%	3.23	0.78	0.83	—
SPS 30A	[6,7,9]	7%	2.1	0.63	0.72	—

* For STAR 200 ϕ/π considering Fig. 14 in [2] we give an average of data for centrality up to 50%.

This function is a good empirical approximation of the individual particle yields. From the functional form of Eq. (1) seen in Fig. 2, one can see that the individual Ξ and ϕ yields change by a factor of ten for Au–Au collisions at 62 GeV studied in the STAR experiment. When we look at the higher energy at STAR and the lower energies at NA49, these individual yields vary even more. However, the ratio Ξ/ϕ (as defined by Eq. (5)) remains within the small range of $0.249 \leq \Xi/\phi \leq 0.304$.

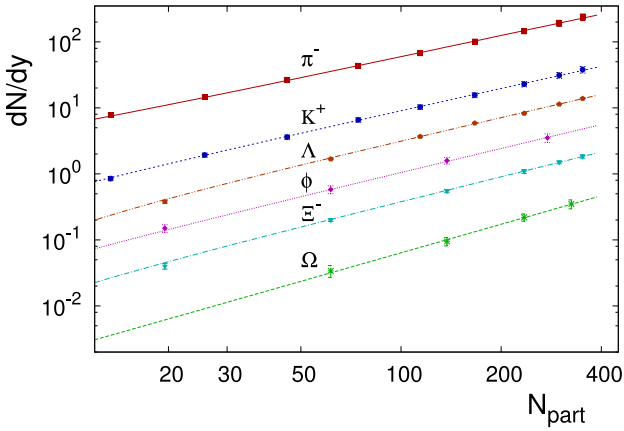

Fig. 2. Data points (full symbols) of particle yields used in the analysis, and their respective fitted centrality dependence.

3. Statistical hadronization considerations

3.1. Equilibration during hadronization

Within the SHM approach particle yields are obtained by evaluating the accessible phase space. The particle density can be written as

$$\frac{N}{V} = g\frac{4\pi}{(2\pi)^3}T^3\sum_{n=1}^{\infty}\frac{\gamma^{\pm n}\lambda^n}{n^3}\left(\frac{nm}{T}\right)^2 K_2\left(\frac{nm}{T}\right), \tag{2}$$

where T is the chemical freeze-out temperature, g is the spin degeneracy factor, γ is the phase space occupancy, λ is the fugacity factor based on the quark content of the given hadron species, and K_2 is the modified Bessel function of the second kind.

There are several popular models of statistical hadronization. They differ by the assumption made about how the quark content of the QGP phase is imaged into the valence quark content of the final hadron state. To begin, one (tacitly) assumes chemical equilibrium of quarks in the quark-gluon plasma phase. This equilibrium condition does not have to (and in fact it is argued in the following that it cannot) become chemical equilibrium of the emerging hadron gas.

To allow for varying degree of chemical equilibration among final state hadrons one introduces the phase space occupancies γ_q and γ_s which control the overall number of quark anti-quark pairs of the light and strange quarks respectively. The fugacity factors λ_q and λ_s control the relative chemical equilibrium (*i.e.*, the relative yields of u, d, s quarks and their respective anti-quarks).

(i) In chemical *equilibrium*, slow hadronization is assumed. During this phase transition, all the flavors of quarks have enough time to re-equilibrate into their respective hadron gas equilibrium $\gamma_q = 1$ and $\gamma_s = 1$ $(q = u, d)$.

(ii) *Semi-equilibrium* model takes into account that lighter quarks could equilibrate faster in hadronization process than strange ones and thus only $\gamma_s \neq 1$, while γ_q is fixed to 1.

(iii) Chemical *non-equilibrium* assumes a rapid hadronization so that not even light quarks have enough time to re-equilibrate. Both strange and light quark phase space occupancies are allowed to adopt values different from unity as appropriate to describe the observed particle yields. Note that when using this most general approach, it is possible to deduce the two earlier models as result of data analysis.

3.2. Multistrange particle production in SHM and model parameters

To be specific, the directly produced yield of ϕ can be expressed as

$$\phi \equiv \frac{N_\phi}{V} = 3\frac{4\pi}{(2\pi)^3} T^3 \sum_{n=1}^{\infty} \frac{\gamma_s^{2n}}{n^3} \left(\frac{nm}{T}\right)^2 K_2\left(\frac{nm}{T}\right). \tag{3}$$

It is important to see how fast this series converges. It depends not only on the mass to temperature ratio, but also on the phase space occupancies and fugacities as they may be greater than unity and appear in increasing powers in the series. To get a sense for how fast this sum converges, let us examine the following case (Table II).

TABLE II

Example of parameters used to study particle densities.

Volume	V	1000 fm^3
Temperature	T	140 MeV
u, d phase space occupancy	γ_q	1.6
s phase space occupancy	γ_s	2.2
Fugacities	$\lambda_{q,s}$	1

When we calculate the partial contributions to the particle yields of interest, we find as shown in Table III, that the heavier the particle is, the faster the sum converges. We have to be careful with less massive particles, such as pions, and even kaons. Considering the first seven terms for pions gives us only 96% of their yield. For Kaons, we have to take the first

two terms to get 99.8% of their yield. However, for particles whose mass $m \gg 100\,\mathrm{MeV}/c^2$, it is sufficient to take the Boltzmann approximation, *i.e.*, just the first term $n = 1$ in Eq. (2):

$$\frac{N}{V} = g\gamma \frac{4\pi}{(2\pi)^3} \lambda m^2 T K_2 \left(\frac{m}{T}\right). \tag{4}$$

One has to be even more careful when using expansion of the Bessel function in m/T which converges much slower.

TABLE III

Contribution of individual terms in the sum Eq. (2) to the particle yields.

	Ξ^-	ϕ	K^-	π^-
$m[\mathrm{MeV/c^2}]$	1321	1020	492	139
m/T	9.4357	7.2857	3.5143	0.99286
N	0.9862	5.6488	51.4969	219.911
Fractions of contributions order by order				
$n = 1$	0.9947	0.9992	0.9692	0.6861
$n = 2$	1.98×10^{-4}	1.04×10^{-3}	2.89×10^{-2}	0.138
$n = 3$	6.46×10^{-8}	1.81×10^{-6}	1.52×10^{-3}	5.74×10^{-2}
$n = 4$	—	—	—	3.14×10^{-2}
...	—	—	—	—
$n = 7$	—	—	—	9.78×10^{-3}

3.3. Ξ/ϕ ratio

Experimentally measured particle yield consists not only of directly produced particles, but also a contribution from heavier resonances decaying into it and thus increasing its apparent yield. In general, the experimental results comprise these contributions. Therefore, we include in our calculations directly produced Ξs and ϕs and the contributions from decays of heavier resonances. The most significant contribution comes from $\Xi^*(1530)$ with spin degeneracy $g = 4$. We use the decay tables as implemented in the SHARE program [10].

Particle yield ratios are very sensitive to the valence quark content and we can take advantage of this by considering specific ratios. One uses ratios since when one takes the same number of hadrons in the numerator as in the denominator, the overall normalization is canceled. We also consider the product of a particle and its antiparticle in order to eliminate the chemical potentials, which are opposite, and therefore the fugacity factors also cancel. Finally, by the choice of hadrons involved, one can change how the ratio depends on the phase space occupancies.

For these reasons, we look first at the generalized ratio of Ξ to ϕ, defined as

$$\frac{\Xi}{\phi} \equiv \sqrt{\frac{\overline{\Xi}^{+}\Xi^{-}}{\phi\phi}} \simeq \frac{\gamma_q\gamma_s^2\lambda_s\lambda_s^{-1}\lambda_q^{1/2}\lambda_q^{-1/2}}{\gamma_s^2\lambda_s\lambda_s^{-1}} f(T, m_\phi, m_\Xi)$$
$$= \gamma_q f(T, m_\phi, m_\Xi)\,. \tag{5}$$

The ratio of Ξ/ϕ is proportional to the light quark phase space occupancy γ_q and a function f of temperature T,

$$f(T, m_\phi, m_\Xi) \simeq \frac{\sum\limits_i g_{\Xi_i} m_{\Xi_i}^2 K_2\left(\frac{m_{\Xi_i}}{T}\right)}{\sum\limits_j g_{\phi_j} m_{\phi_j}^2 K_2\left(\frac{m_{\phi_j}}{T}\right)}\,, \tag{6}$$

which is determined by degeneracies g_i and masses of the hadrons contributing to the yields and over which we sum using the Boltzmann approximation.

As evident from Eq. (2), the effect of quantum statistics is decreasing with the hadron mass m when compared to the freeze-out temperature T. We calculated the magnitude of this effect to be 0.25% for the Ξ/ϕ ratio — it is therefore negligible. One has to remember that the formula for the residual function Eq. (6) does not account for strong decays in which flavor content is redistributed, nor does reflect any possible weak decays influencing the yields in question.

Global fits [11–13] of the systems under consideration show that all these systems hadronize at the same temperature T in the non-equilibrium model. This, together with the observed constant ratio of Ξ/ϕ, implies common hadronization conditions for all the systems studied. Another immediate implication is that the light quark phase space occupancy γ_q is constant and has the same value for all the energies, centralities and systems studied.

To obtain the results presented here we actually use the SHARE program [10]. We consider several values of the Ξ/ϕ ratio and plot the results in the γ_q–T plane in Fig. 3. In combination with the global fit results, there are two possible regions to look for possible hadronization conditions. The first region corresponds to light quarks being in chemical equilibrium. This is represented by $\gamma_q = 1$, and from Fig. 3, we see temperature $T \simeq 170$ MeV. To locate the second region, we allow for fast hadronization and relax light quark phase space occupancy $\gamma_q \neq 1$. When varying the magnitude of γ_q, one has to remember that there is a critical value of this parameter for which pions begin to form a Bose–Einstein condensate. This critical value is given by the mass of the lightest, non-strange meson (π^0) by

$$\gamma_q < \gamma_q^{\rm crit} \equiv \exp\left(\frac{m_{\pi^0}}{2T}\right). \tag{7}$$

This is shown as an upper limit in Fig. 3.

In conclusion of this analysis, we observe that it is possible for different reaction systems to occupy different values of T and γ_q along the solid black line in Fig. 3. However, much more plausible interpretation is that all reaction systems considered hadronize at the same set of T, γ_q. This result is strongly supported by the global fit of all hadron yields we performed and in which near critical value of $\gamma_q \simeq 1.6$ is favored. Fig. 3 then implies temperature $T \simeq 140\,\mathrm{MeV}$.

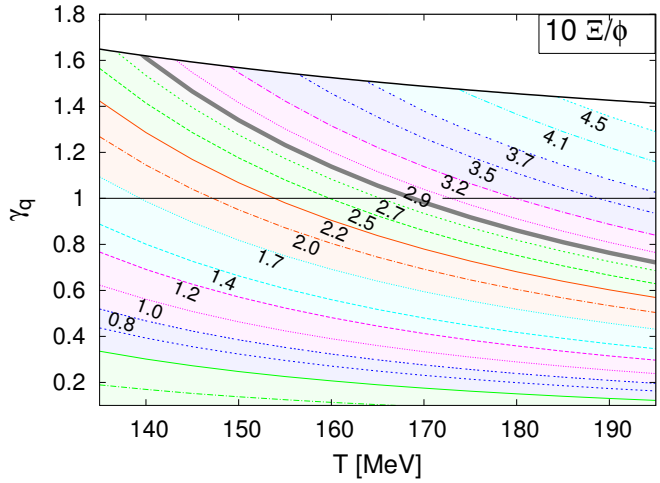

Fig. 3. Lines of a constant ratio $10 \times \Xi/\phi \in [0.8, 4.5]$ (as defined in Eq. (5)) in the T–γ_q plane. The lines for $\gamma_q = 1$ and $\gamma_q = \gamma_q^{\rm crit}$ are presented by solid black lines. The thick gray line represents the average result of all SPS and RHIC.

3.4. Hadronization of strangeness

In the previous subsection, we found that the ratio Ξ/ϕ is proportional to light quark phase space occupancy γ_q. To study strangeness occupancy γ_s we have to identify a ratio proportional to γ_s. By the same reasoning as before, we are motivated to examine the ratio of Ξ to K defined as

$$\frac{\Xi}{K} \equiv \sqrt{\frac{\overline{\Xi}^+ \Xi^-}{K^+ K^-}} = \gamma_s f_1(T). \tag{8}$$

It is evident from both Table I and Fig. 1 that Ξ/K is not constant. The Au–Au, $\sqrt{s_{NN}} = 62.4$ GeV, RHIC data which inspired this study show a systematic variation with a factor of 1.5 difference between central and peripheral collisions. When we consider the other systems and energies studied, the factor increases to more than two. We believe this is entirely due to variation in γ_s since, as we argued, that T is constant.

When γ_s is allowed to vary, we have to remember, especially in the view of the expected conditions at LHC where γ_s could turn out to be large, that there is also a critical value of γ_s. It turns out that it is the η meson ($\eta = 0.45(u\bar{u} + d\bar{d}) + 0.55 s\bar{s}$) which is the first to condensate when γ_s increases. The critical value for γ_s is a function of temperature and can be obtained from the condition

$$0.45\gamma_q^2 + 0.55\gamma_s^2 = \exp\left(\frac{m_\eta}{T}\right) . \tag{9}$$

The critical value of γ_s is not as sensitive to γ_q as it is to temperature. For the two scenarios discussed, $T = 140\,\mathrm{MeV}$ and $T = 170\,\mathrm{MeV}$, we get the critical value of $\gamma_s^{\mathrm{crit}} = 9.47$ and $\gamma_s^{\mathrm{crit}} = 6.68$, respectively.

4. Predictions

4.1. General considerations

We have argued in the last section, that the temperature is constant for all the systems, and we have attributed the change in relative yield of Ξ and K to the change in γ_s. This implies that the strangeness initially present in the fireball of QGP does not have enough time to re-equilibrate during the hadronization, and the strange phase space in the hadron gas phase can be under- or over-populated. As a consequence, we conclude that chemical equilibrium model *(i)* in Subsection 3.1, which assumed both light and strange quarks to be in chemical equilibrium after hadronization, is no longer a viable description of particle yields in heavy-ion collisions.

With the range of γ_q, γ_s and T established by measuring Ξ/ϕ and Ξ/K, we can now predict the ratios of particles which are harder to observe experimentally. According to the quark content of the particles in question, we establish how their ratio depends on phase space occupancies and with that predict the behavior and possible values of their ratio.

Both the ratios Ξ/K and Ω/ϕ are proportional to γ_s. In the top section of Fig. 4 we show fixed values of Ξ/K and the band of experimental data for this ratio in the T–γ_s plane. In the bottom frame of Fig. 4 we show the corresponding Ω/ϕ ratio and find a narrow range

$$\frac{\Omega}{\phi} \equiv \sqrt{\frac{\Omega^-\overline{\Omega}^+}{\phi\phi}} \in \left\langle 5.5 \times 10^{-2}, 7.0 \times 10^{-2} \right\rangle . \tag{10}$$

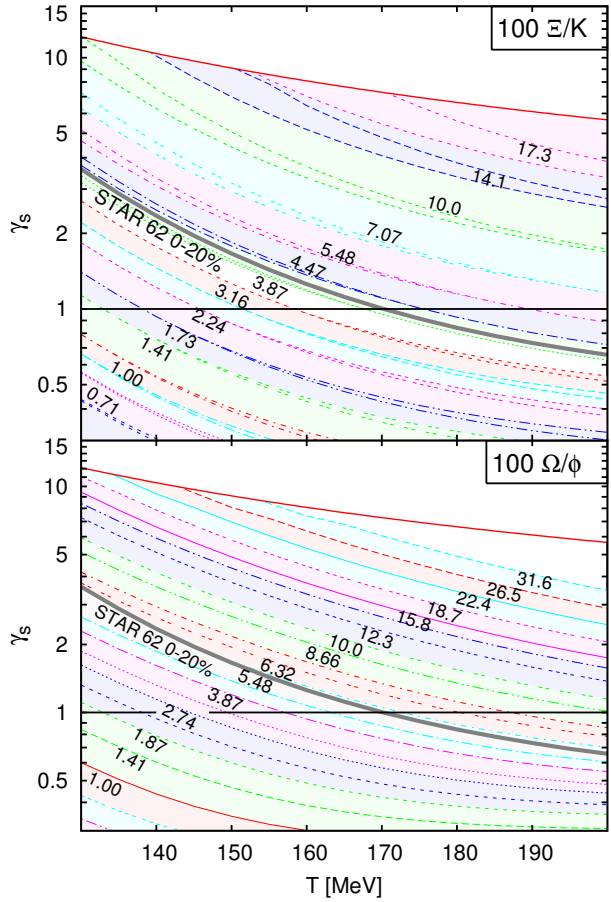

Fig. 4. Lines of constant ratio Ξ/K (top) and Ω/ϕ (bottom). Experimental data from most central 0–20% STAR 62 are indicated by a thick line (top), and is assumed in the bottom frame as a prediction. See text for more detail.

Similarly, with temperature T, γ_q and γ_s constrained to a small range of values, we can predict other ratios of particles, such as ϕ/π or Ξ/π (see Fig. 1) defined by

$$\frac{\Xi}{\pi} \equiv \sqrt{\frac{\Xi^-\overline{\Xi}^+}{\pi^-\pi^+}} \propto \frac{\gamma_s^2}{\gamma_q}, \qquad \frac{\phi}{\pi} \equiv \sqrt{\frac{\phi\phi}{\pi^-\pi^+}} \propto \left(\frac{\gamma_s}{\gamma_q}\right)^2, \tag{11}$$

which are both very sensitive to the amount of strangeness in the emerging hadron gas due to their dependence on γ_s^2.

4.2. LHC conditions

One very simple and solid prediction we can make based on the universality of the results for Ξ/ϕ is that $\Xi/\phi = 0.28 \pm 10\%$ at LHC too. This universal hadronization condition for T, γ_q has been observed so far in both SPS and RHIC results. We strongly believe that this yield will be observed in heavy ion collisions at LHC.

We also expect considerably greater absolute yield of ϕ at LHC, since one can anticipate that there is a greater strange quark pair density production because of more extreme initial conditions [14]. We found in a kinetic exploration of strangeness production that the strangeness over entropy ratio at LHC is at least $s/S \simeq 0.037$. This implies, as shown in [15], that the ratio of $\gamma_s/\gamma_q \simeq 1.55$. We use this value in our further LHC predictions. Here we note that since the size of reaction volume changes, as does baryon and strangeness content, several SHM parameters such as $V, \gamma_s, \lambda_q, \lambda_s$ are expected to change. Thus the hadronization universality only refers to T, γ_q.

We show the required value of γ_s as a function of the measured value of ϕ/π in Fig. 5 for both chemical semi-, and non-equilibrium. Also we show (colored) bands of data from different experiments and also a prediction for LHC results. It is evident from the figure that the temperature does not have a great effect on this ratio when we fix $\gamma_q = 1$, a very fortuitous result — the increase of ϕ-yield with T is nearly compensated by increase in π-yield. Thus, if at LHC $\phi/\pi > 0.03$ we can be sure that irrespective of the model of hadronization the value of $\gamma_s > 1$.

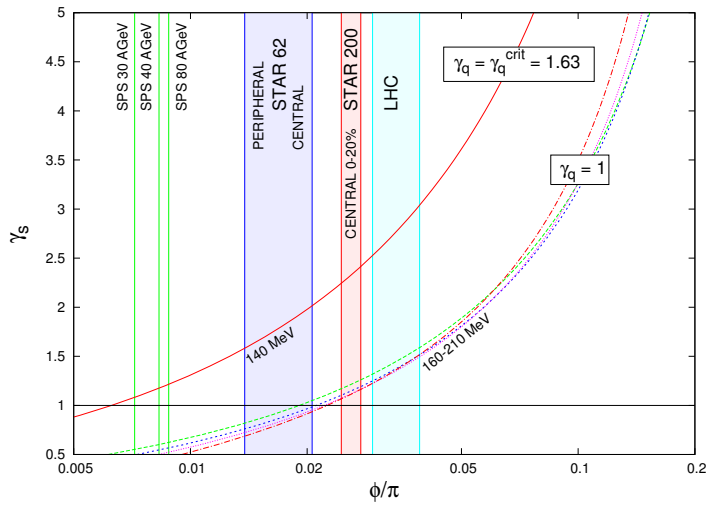

Fig. 5. γ_s as a function of the relative ϕ/π yield Eq. (11) in two hadronization scenarios, see text. The horizontal solid black line shows the chemical equilibrium with $\gamma_s = 1$. For experimental data see Table I.

$\gamma_s > 1$ cannot be build up from a small initial value in hadron based strangeness production since chemical equilibrium is reached at $\gamma_s = 1$. On the other hand, when the source of hadrons is a strangeness rich initial phase, such as chemically equilibrated quark-gluon plasma, hadronization can lead to phase space overpopulation in final state. This is true in particular for a fast hadronization process, in which strangeness content does not have time to re-annihilate.

5. Conclusions

The experimental results from SPS and RHIC provided an important observation, that the ratio Ξ/ϕ is nearly constant for wide range of energies, centralities and even across different systems, while the individual yields change by more than an order of magnitude. As this ratio is governed by light quark phase space occupancy γ_q, and hadronization temperature T, than these conditions are very likely universal for all the experiments. This universality in regard to T, γ_q is strongly supported by global data fits [13, 16].

A different ratio, Ξ/K, which is proportional to strange phase space occupancy γ_s, changes by a factor of 2, which implies that γ_s changes significantly between different experiments and centralities. Thus, we learn that the full chemical equilibrium hadronization is not a viable model.

We further find that some experimentally observed yields of multistrange hadrons, such as ϕ, are only compatible with $\gamma_s > 1$. For this to happen, we require strangeness rich initial phase (quark-gluon plasma) and fast hadronization, so that strangeness abundance does not have enough time to re-equilibrate during hadronization.

Our study allowed us to predict certain particle ratios for which precise data is not available at present experiments and for the upcoming LHC. For example, we expect $\Omega/\phi \in \langle 5.5 \times 10^{-2}, 7.0 \times 10^{-2} \rangle$ at RHIC 62 GeV. We expect the ratio Ξ/ϕ to remain in the same range of values at LHC as it has been measured at SPS and RHIC, *i.e.*, $\Xi/\phi \in \langle 0.249, 0.304 \rangle$.

Laboratoire de Physique Théorique et Hautes Energies, LPTHE, at University Paris 6 and 7 is supported by CNRS as Unité Mixte de Recherche, UMR7589. This work was supported by the grant LC07048 and LA 316 from the Czech Ministry of Education and the grant from the US Department of Energy, DE-FG02-04ER41318.

REFERENCES

[1] M. Petran, J. Rafelski, *Phys. Rev.* **C82**, 011901 (2010) [arXiv:0912.1689[hep-ph]].

[2] B.I. Abelev *et al.* [STAR Collaboration], *Phys. Lett.* **B673**, 183 (2009) [arXiv:0810.4979 [nucl-ex]].

[3] J. Speltz, http://drupal.star.bnl.gov/STAR/theses/ph-d/jeff-speltz

[4] B.I. Abelev *et al.* [STAR Collaboration], *Phys. Rev.* **C79**, 034909 (2009) [arXiv:0808.2041 [nucl-ex]].

[5] J. Adams *et al.* [STAR Collaboration], *Phys. Rev. Lett.* **98**, 062301 (2007) [arXiv:nucl-ex/0606014].

[6] C. Alt *et al.* [NA49 Collaboration], *Phys. Rev.* **C78**, 044907 (2008) [arXiv:0806.1937 [nucl-ex]].

[7] C. Alt *et al.* [NA49 Collaboration], *Phys. Rev.* **C78**, 034918 (2008) [arXiv:0804.3770[nucl-ex]].

[8] S.V. Afanasiev *et al.* [NA49 Collaboration], *Phys. Rev.* **C66**, 054902 (2002) [arXiv:nucl-ex/0205002].

[9] C. Alt *et al.* [NA49 Collaboration], *Phys. Rev.* **C77**, 024903 (2008) [arXiv:0710.0118[nucl-ex]].

[10] G. Torrieri, *et al., Comput. Phys. Commun.* **167**, 229 (2005) [arXiv:nucl-th/0404083].

[11] J. Rafelski, J. Letessier, G. Torrieri, *Phys. Rev.* **C72**, 024905 (2005) [arXiv:nucl-th/0412072].

[12] J. Rafelski, J. Letessier, *J. Phys. G* **36**, 064017 (2009) [arXiv:0902.0063[hep-ph]].

[13] J. Letessier, J. Rafelski, *Eur. Phys. J.* **A35**, 221 (2008) [arXiv:nucl-th/0504028].

[14] J. Letessier, J. Rafelski, *Phys. Rev.* **C75**, (2007) 014905 [arXiv:nucl-th/0602047].

[15] I. Kuznetsova, J. Rafelski, *Eur. Phys. J.* **C51**, 113 (2007) [arXiv:hep-ph/0607203].

[16] J. Rafelski, J. Letessier, *PoS* **CONFINEMENT8**, 111 (2008) [arXiv:0901.2406[hep-ph]].